Chapter 5

Pressure Characteristics from Different Configurations

In chapter 3, we discussed the characteristics of the simulated incident flow by its statistical parameters. In chapter 4, wavelet analysis is applied to characterize the velocity field of the simulated turbulence in the eight configurations. In this chapter, we discuss how the pressure varies for these configurations. Such variations are important because they could be used as a basis for establishing flow parameters that would allow for the best simulation of full-scale pressure loads. The relation between parameters, as presented in chapter 3, and the corresponding pressure characteristics have been studied by many researchers, such as Tieleman et al[1999]. In this work, we will focus more on the relation between pressure characteristics and the wavelet parameters representing time-varying characteristics.

The pressure comparison presented in this chapter is based on pressure coefficients Cp_{mean} and Cp_{min} at each pressure tap location. These quantities are based on sixteen repeats for every flow configuration. Four configurations are examined. These are configurations #4, #6, #7 and #8. Details on these configurations have been presented in chapter 2. Four sets of roof pressures, each

consisting of 8 pressure taps were investigated. These taps are placed along a line parallel to the long side of the model and at a distance x/H=0.663 from the roof corner for and azimuth angle of 180 degrees. These eight taps are placed at distances y/H equal to 0.039, 0.091, 0.169, 0.247, 0.325, 0.403, 0.559, 0.715, and represented by number 50900, 50902, 50903, 50904, 50905, 50907, 50909 and 50927 respectively. The sampling frequency is 2000Hz, and the sampling period is 20 seconds. More details on the experimental setup are given in Tieleman et al. [1999].

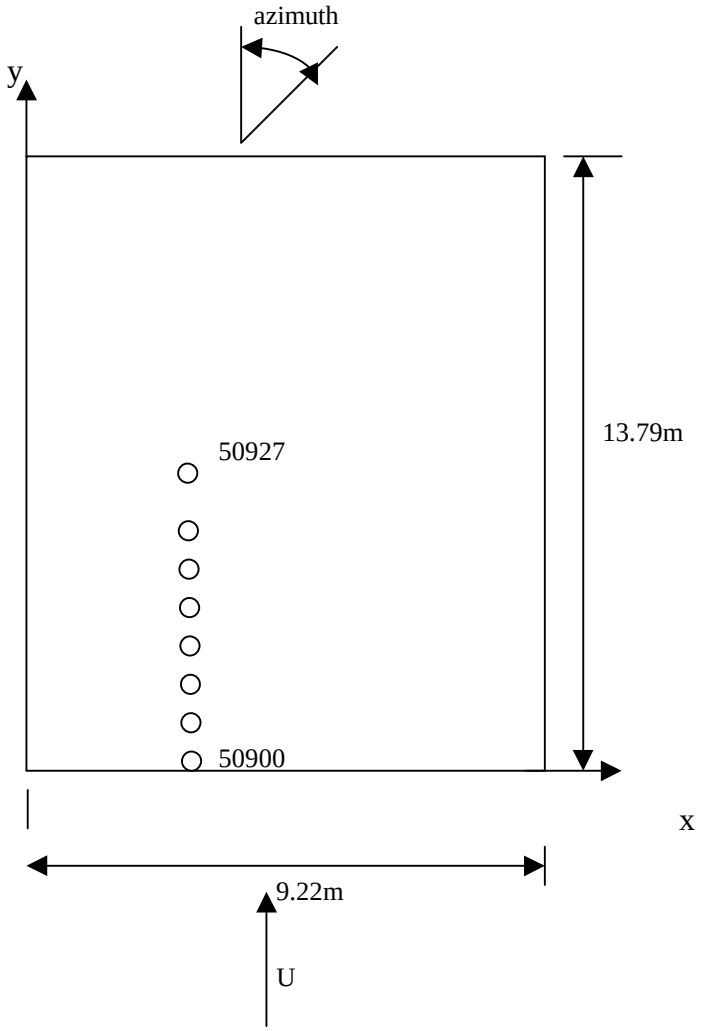

Figure 5.1 Tap locations on the roof

5.1 Pressure coefficients

Values of the minimum of $C_{p_{min}}$ from 16 repeats are shown in figures 5.2 to 5.5 for configurations #4, #6, #7 and #8 respectively. The results show that in all configurations, $C_{p_{min}}$ varies considerably. These variations are larger near the leading edge of the building. More quantitative details of these variations are shown in figure 5.6. These variations are given in terms of minimum of $C_{p_{min}}$ (figure 5-6a), range of $C_{p_{min}}$ (figure 5-6b). The results show that all taps of configuration #6 consistently capture much smaller pressure peaks, as indicated by lower absolute values of negative $C_{p_{min}}$. In addition, figure 5.6b shows that, the range of measured $C_{p_{min}}$ over sixteen repeats of configuration #6 is consistently smaller than other configurations at all locations, except for tap #5. A subplot of the minimum of $C_{p_{mean}}$ of sixteen repeats indicate again that configuration #6 has relatively smaller pressure peaks on average. All the experiments show that, in configuration #6, the pressure peaks are small relative to the other simulations.

The minimum pressure coefficients in configuration #7 show also some distinct features. The minimum of $C_{p_{mean}}$ of the sixteen repeats of configuration #7 consistently reveals stronger negative pressure peaks at all roof locations than the other three configurations. However, for the minimum of $C_{p_{min}}$ and range of $C_{p_{min}}$, the result of the comparison with other configurations is dependent on the tap's location. At y/H= to 0.039 and 0.091, configuration #7 has much stronger negative pressure peaks than in other configurations. At the same time, the variation of $C_{p_{min}}$ of the sixteen repeats extends over a larger range than for the

other configurations. At all other locations, the minimum of Cp_{min} doesn't have distinct difference from configurations #4 and #8.

The above measurements indicate that, configuration #7 could generate the strongest negative pressure peak; however, it has the largest variations over sixteen repeats especially near the leading edge. In terms of the minimum of Cp_{mean}, figure 5.6c shows that configuration #7 causes the largest minimum for Cp_{mean}. Configurations #4 and #8 have about the same values and configuration #6 produces consistently the lowest value for Cp_{mean}. These observations are true at all locations. When considering the minimum variations of Cp_{min} over sixteen repeats, the results are not as clear. Near the leading edge, at y/H equal to 0.039 and 0.091, the results show that configurations #4 and #7 have the highest (in absolute measure) Cp_{min}; yet they have a much larger range of variations. Configuration #6 results in the lowest (in absolute measure) Cp_{min} as well as the lowest range of variations. The difference between measured values for minimum of Cp_{min} reaches as much as 85% between configuration #6 and configurations #4 and #7. At all other locations, the minimum values of Cp_{min} and range of variations are closer to each other in all configurations.

The above analysis shows the effect of different configurations on varying pressure peak characteristics. When evaluating these results along with the wavelet parameters presented in chapter 4,interesting relations between wavelet parameters and pressure characteristics are revealed. Based on the wavelet coefficients presented in in figure 4.12, 4.14, 4.15 and 4.16, one can state that, up to scale with m=5 (≤1.95Hz), the wavelet coefficients of the u- component in configuration #7 are consistently smaller than those of configuration #6, and this

difference is especially big for very large scales with m=1 and 2 (≤0.244 Hz). For intermediate scales, as represented by m=6 to 9 (3.91 to 31.3 Hz), values of the wavelet coefficients in both configurations are about the same. For smaller scales, m=11 and 12 (125 to 250Hz), it is shown that, configuration #7 consistently has higher values than configuration #6. Results of the v- component comparison indicates similar characteristics. However, for the v- component, the degree of the difference between large scales up to m=5 (≤ 1.95Hz) is not as large as it is with the u- component.

From the above observations, it can be concluded that higher wavelet coefficients in smaller scales in both u- and v- may result in stronger negative pressure peaks. A consistently higher percentage energy distribution among small scales may also contribute to strong negative pressure peaks. The high intermittency factor may have some relation to the non-stationery characteristic of the simulated flow as it is connected with larger variation of pressure parameters over many repeats. Comparisons made for configurations #6 and #8 also show similar conclusions.

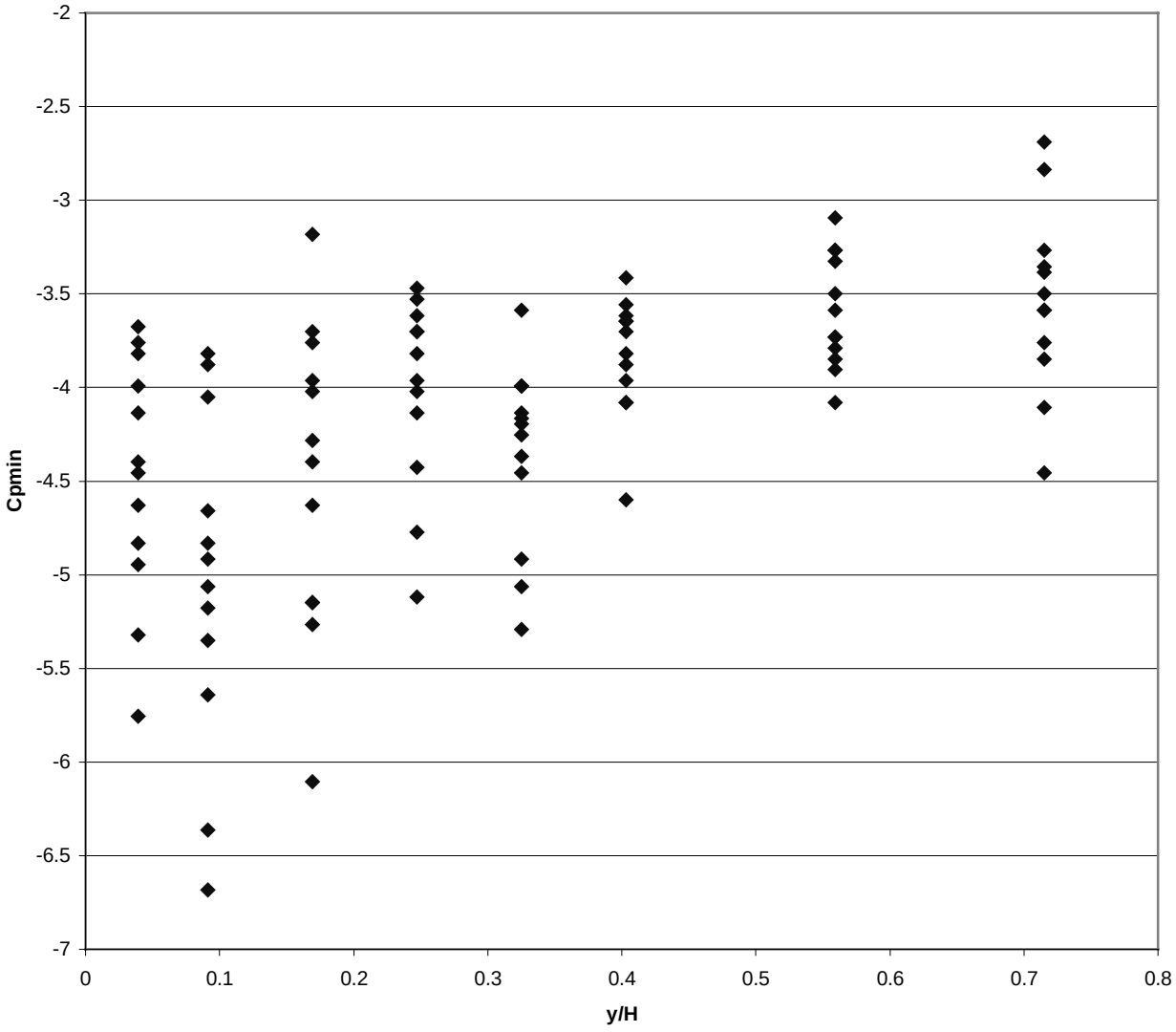

Figure 5.2 C$p_{\min}$ versus distance from leading edge of configuration #4 over 12 repeats

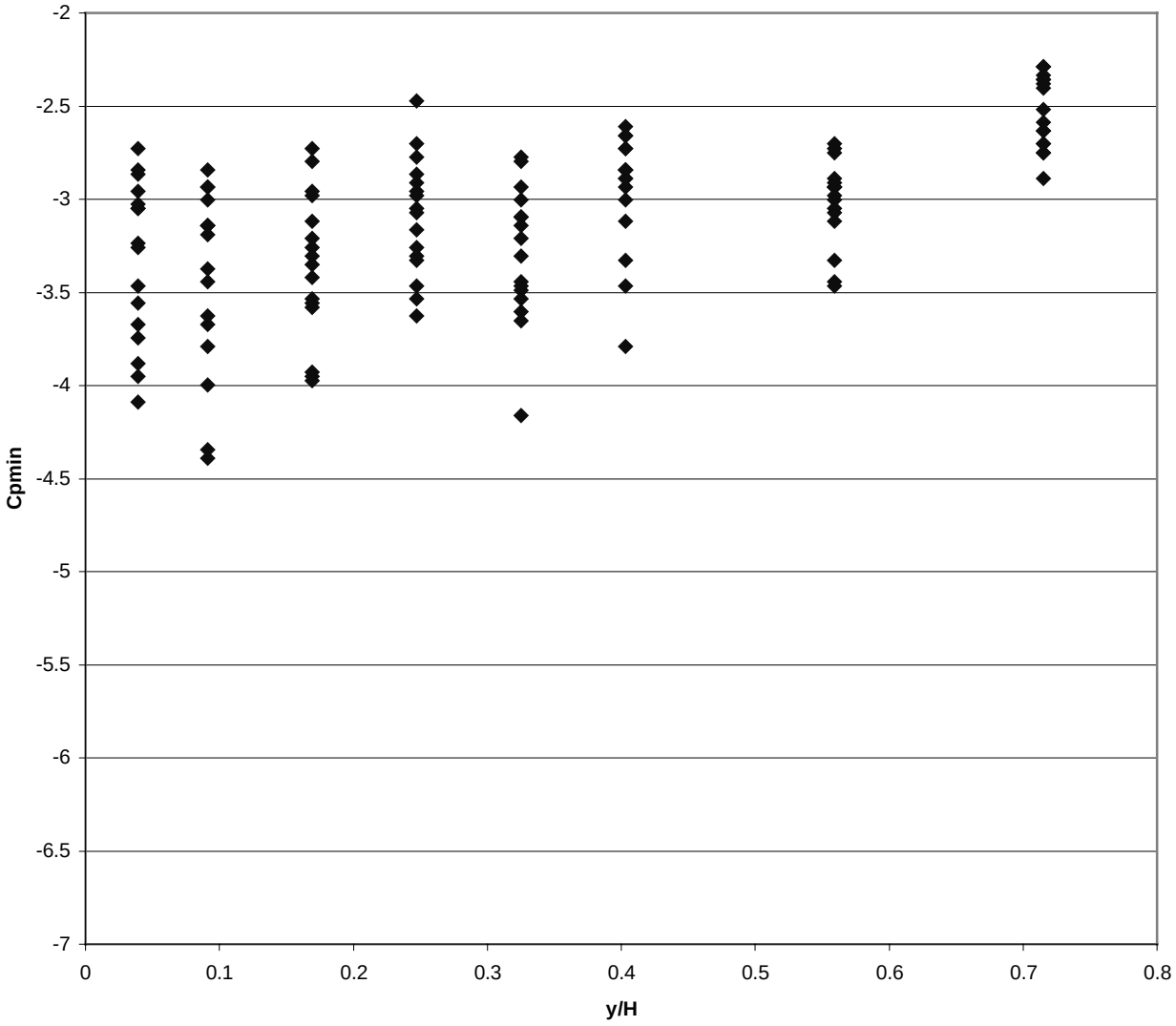

Figure 5.3 C$p_{\min}$ versus distance from leading edge of configuration #6 over 16 repeats

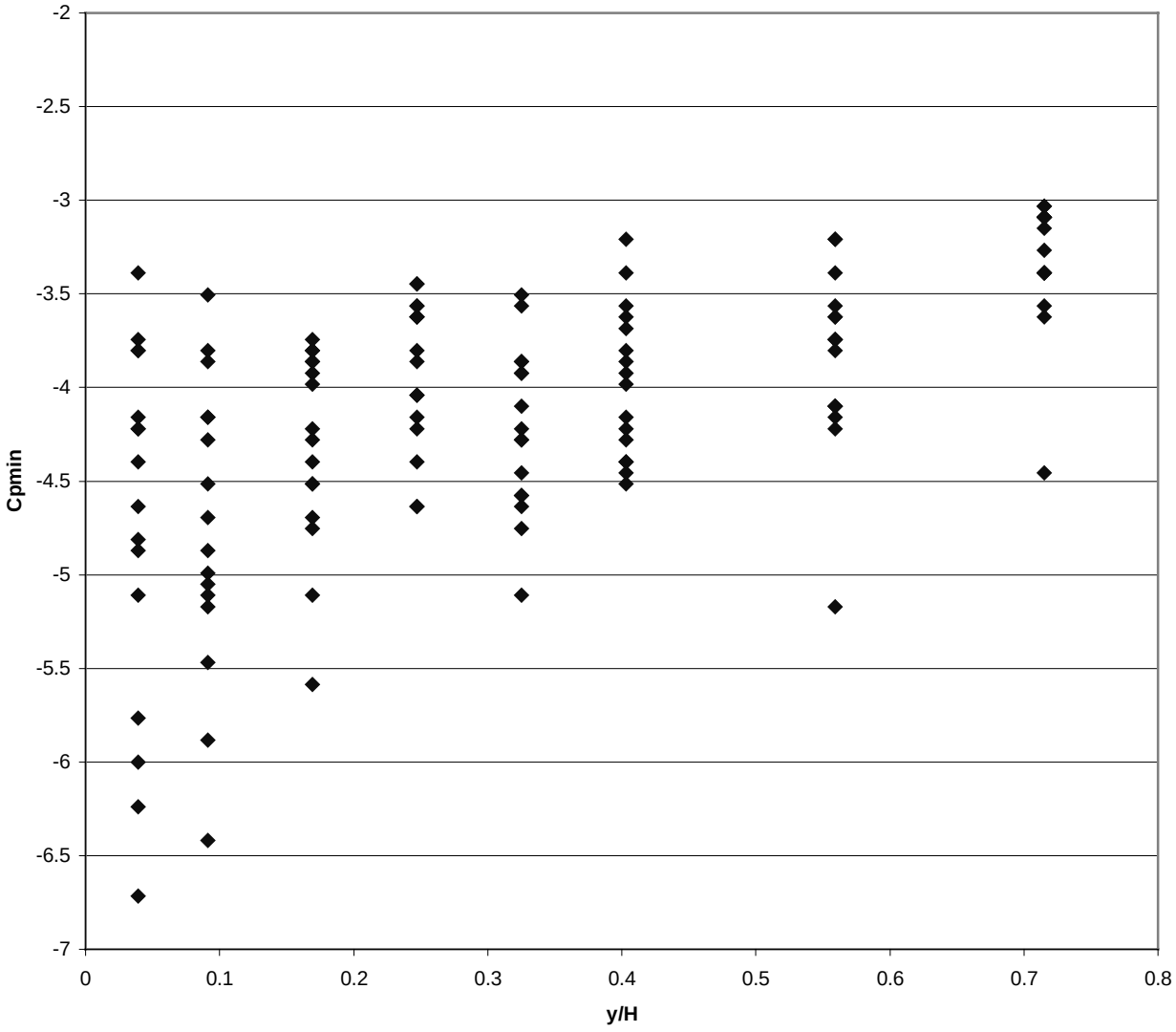

Figure 5.4 C$p_{\min}$ versus distance from leading edge of configuration #7 over 16 repeats

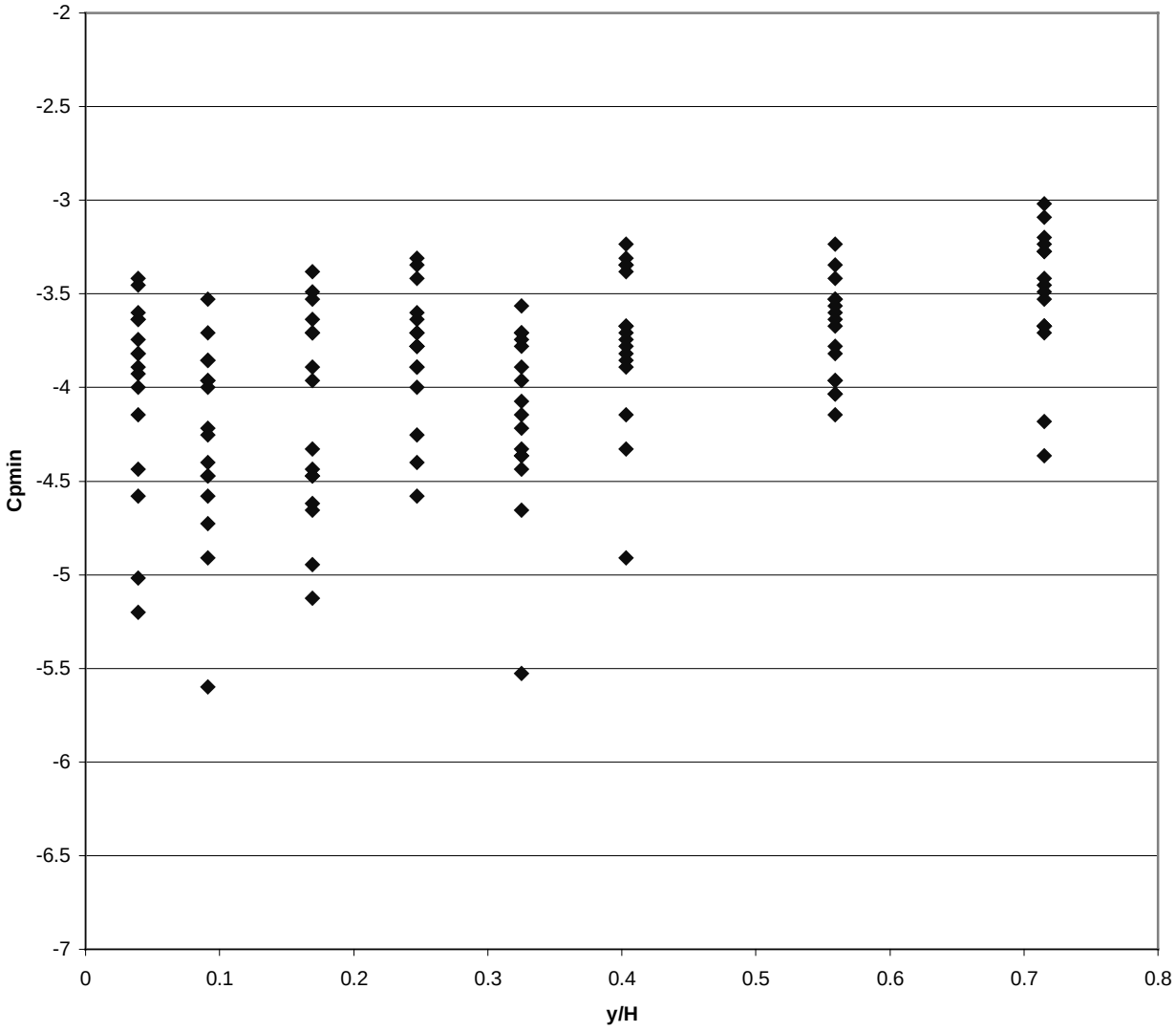

Figure 5.5 C$p_{\min}$ versus distance from leading edge of configuration #8 over 16 repeats

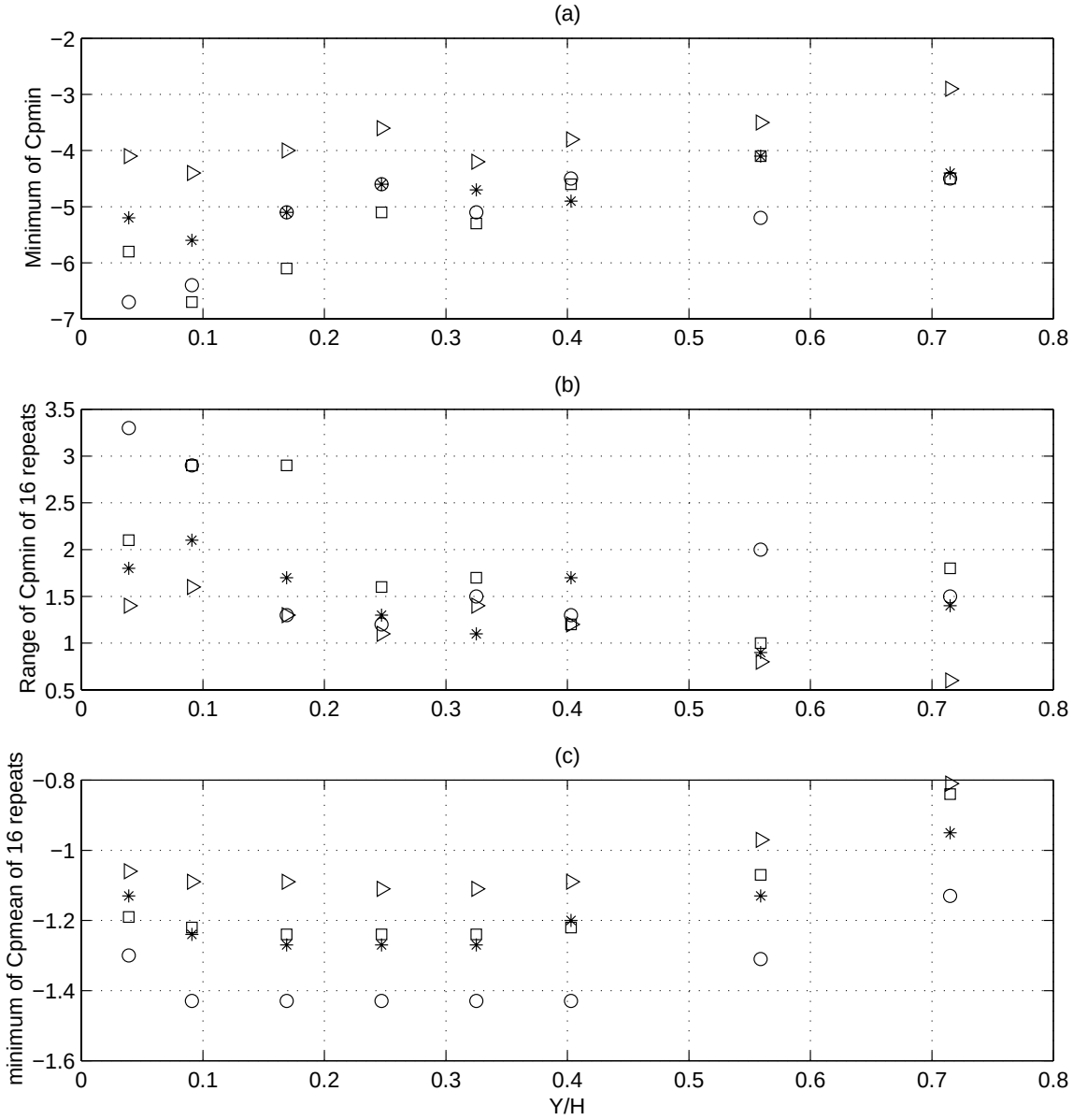

Figure 5.6 Pressure peak coefficients of configurations #4 --- □, #6 --- ▷ , #7 --- o and #8 --- *:
(a)Minimum of Cp_{min} (b) Range of Cp_{min} over 16 repeats (c) Minimum of Cp_{mean} over 16 repeats